Design and Analysis of Second-order Steerable Differential Microphone Arrays

Xiaoguang Wu[1,2] *and Huawei Chen*[2]

[1,2] College of Computer Science and Technology,
Nanjing Tech University, Nanjing 211816, China
[2] College of Electronic and Information Engineering,
Nanjing University of Aeronautics and Astronautics, Nanjing 210016, China

ABSTRACT

Second-order differential microphone arrays (DMAs) are one of the most commonly used DMAs in practice due to the sensitivity of higher-order DMAs to microphone mismatches and self-noise. However, conventional second-order DMAs are non-steerable with their mainlobe orientation fixed along the array endfire direction, which are not applicable to the case where sound sources may move around a large angular range. In this paper, we propose a design of second-order steerable DMAs (SOSDAs) using seven microphones. The design procedure is discussed, followed by the theoretical analysis on directivity factor and white noise gain of the proposed SOSDAs. Numerical examples are shown to demonstrate the effectiveness of the proposed design and its theoretical analysis.

***Index Terms*—** Differential microphone array, steerable beamforming, superdirective beamforming.

1. INTRODUCTION

Microphone arrays have attracted great interest in audio and speech processing, with applications such as teleconferencing, hands-free telephony and hearing aids, among many others. A variety of designs for microphone arrays have been proposed in the past decades. Among them, differential microphone Arrays (DMAs) whose responses are related to spatial derivatives of an acoustic pressure field, offer some advantages over their additive counterparts, e.g., the delay-and-sum arrays [1]. Comparatively, DMAs can achieve higher directivity and frequency-invariant beampatterns with a small array size.

Due to the fact that higher-order DMAs are more sensitive to microphone mismatches and self-noise, lower-order DMAs, i.e., first- and second-order DMAs, are mostly studied in practice [2–8]. It is noted that the mainlobe orientation of conventional first- and second-order DMAs is fixed and non-steerable, i.e., along the array endfire direction. In some practical applications, however, sound sources of interest may move around a large angular range, and it limits the use of the conventional non-steerable DMAs. To address the problem, some design approaches for *first-order* steerable DMAs have been proposed in the literature [9–13]. In this work, we present a design and related analysis of *second-order* steerable DMAs (SOSDAs), which is inspired by the previous works [11–13]. The proposed SOSDAs consist of seven microphones which are coplanar. Compared with the first-order steerable DMAs [11–13], the use of additional three microphones enables beam steering over the entire 360° azimuthal angles with a constant directivity factor (DF). Theoretical analysis on DF and white noise gain (WNG) is also presented. We evaluate the effectiveness of the proposed design via some numerical examples.

This work was supported by the National Natural Science Foundation of China under Grant No. 61471190.

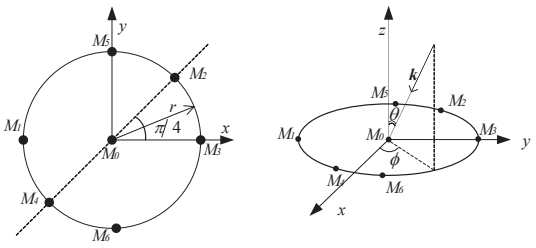

Fig. 1. Array configuration of the proposed second-order steerable DMAs.

2. PROPOSED DESIGN

2.1. Array Configuration

The array configuration of the proposed SOSDAs, consisting of seven microphones $M_0, M_1, \cdots, M_6$, is shown in Fig. 1, where microphones $M_1, M_2, \cdots, M_6$ are located on a circle with a radius of r and microphone M_0 is placed at the center of the circle. Compared with the first-order steerable differential microphone arrays (FOSDAs) [11–13], herein three more microphones have been employed, i.e., M_0, M_2, and M_4.

For a unit-amplitude harmonic plane-wave impinging on

ISBN 978-0-9928626-7-1 © EURASIP 2017

the array with frequency f, and incident angle (θ, ϕ), where $\theta \in [0, \pi]$ and $\phi \in [0, 2\pi]$ denote the elevation and azimuth angles, respectively, the signal received by microphone M_i can be expressed as

$$E_i = \exp\left[j\omega t + j\omega r \sin\theta \left(p_{x_i} cos\phi + p_{x_i} sin\phi\right)/c\right] \quad (1)$$

where $\omega = 2\pi f$, t denotes the time, p_{x_i} and p_{y_i} represent the x- and y- coordinates of microphone M_i, c is the speed of sound, and $j = \sqrt{-1}$. In the following, we assume that $\omega r/c \ll 1$.

2.2. Design of Second-Order Steerable DMAs

The implementation structure of the proposed SOSDAs is shown in Fig. 2. The key to the structure lies in the three branches constructing the monopole $\overline{E}_m$ (the lower branch in Fig. 2), the first-order steered dipole $\overline{E}_{1d}^{\varphi_s}(\theta, \phi)$ (the middle branch in Fig. 2), and the second-order steered dipole $\overline{E}_{2d}^{\varphi_s}(\theta, \phi)$ (the upper branch in Fig. 2), where $\varphi_s \in [0, 2\pi)$ denotes the desired mainlobe orientation.

Proposition 1: The array response of the SOSDAs is corresponding to that of the conventional non-steerable second-order DMAs with its mainlobe rotated to φ_s. Mathematically, we have

$$\begin{aligned}
&\overline{E}_{\alpha_1,\alpha_2}^{\varphi_s}(\theta, \phi) \\
&= (1 - \alpha_1 - \alpha_2)\overline{E}_m(\theta, \phi) + \alpha_1 \overline{E}_{1d}^{\varphi_s}(\theta, \phi) + \alpha_2 \overline{E}_{2d}^{\varphi_s}(\theta, \phi) \\
&\approx (1 - \alpha_1 - \alpha_2) + \alpha_1 \cos(\phi - \varphi_s)\sin\theta \\
&\quad + \alpha_2 \cos^2(\phi - \varphi_s)\sin^2\theta.
\end{aligned} \quad (2)$$

where $\overline{E}_{\alpha_1,\alpha_2}^{\varphi_s}(\theta, \phi)$ denotes the array response of the SOSDAs, $\alpha_1, \alpha_2 \in [0, 1]$ are the directivity controlling parameters. Typically, when $\alpha_1 = \alpha_2 = 1/2$ it is corresponding to the second-order cardioid, and when $\alpha_1 = 1/3$, $\alpha_2 = 5/6$ corresponding to the second-order hypercardioid.

As a special case, when $\varphi_s = 0^\circ$ it follows that (2) will degenerate into the array response of conventional second-order DMAs.

2.2.1. Construction of Monopole

The array response of the monopole can be expressed as

$$\begin{aligned}
\overline{E}_m(\theta, \phi) &= \frac{1}{7}\sum_{i=0}^{6} E_i \\
&= \frac{1}{7}\left(2\cos\Theta_{31} + 2\cos\Theta_{24} + 2\cos\Theta_{56} + 1\right)
\end{aligned} \quad (3)$$

where $\Theta_{31} = \Omega \sin\theta\cos\phi$, $\Omega = \omega r/c$, $\Theta_{24} = \Omega\sin\theta \times \cos(\phi - \pi/4)$, $\Theta_{56} = \Omega\sin\theta\cos(\phi - \pi/2)$. For the case $\Omega \ll 1$ (note that $\cos x \approx 1$ for small value of x), it can be easily deduced that $\overline{E}_m(\theta, \phi) \approx 1$.

2.2.2. Construction of First-Order Steered Dipole

The first-order steered dipole is constructed via two orthogonal first-order dipoles oriented toward 0 and $\pi/2$ radians, respectively, i.e.,

$$E_{1d}^{0}(\theta, \phi) = E_3 - E_1 = e^{j\Theta_{31}} - e^{-j\Theta_{31}} = 2j\sin\Theta_{31}. \quad (4)$$

$$E_{1d}^{\pi/2}(\theta, \phi) = E_5 - E_6 = e^{j\Theta_{56}} - e^{-j\Theta_{56}} = 2j\sin\Theta_{56}. \quad (5)$$

For $\Omega \ll 1$, we have $\sin\Theta_{31} \approx \Theta_{31}$, $\sin\Theta_{24} \approx \Theta_{24}$. Thus, by normalization the array response of the first-order steered dipole can be expressed as

$$\begin{aligned}
\overline{E}_{1d}^{\varphi_s}(\theta, \phi) &= \frac{1}{j\omega}\frac{c}{2r}\left[\cos\varphi_s E_{1d}^{0}(\theta, \phi) + \sin\varphi_s E_{1d}^{\pi/2}(\theta, \phi)\right] \\
&\approx \cos(\phi - \varphi_s)\sin\theta
\end{aligned} \quad (6)$$

where $1/(j\omega)$ is an integrator to obtain a frequency-invariant dipole response and $c/(2r)$ is an extra compensation term to normalize the dipole.

2.2.3. Construction of Second-Order Steered Dipole

To construct a second-order steered dipole, we need to employ three second-order dipoles with their mainlobes oriented toward 0, $\pi/4$ and $\pi/2$ radians, respectively. The second-order dipole oriented toward 0 radians can be constructed by

$$\begin{aligned}
E_{2d}^{0}(\theta, \phi) &= 2E_0 - E_1 - E_3 = 2 - e^{-j\Theta_{31}} - e^{j\Theta_{31}} \\
&= 2\left(1 - \cos\Theta_{31}\right) = 4\sin^2\left(\Theta_{31}/2\right)
\end{aligned} \quad (7)$$

Similarly, the remaining second-order dipoles oriented toward $\pi/4$ and $\pi/2$ radians can be constructed according to

$$E_{2d}^{\pi/4}(\theta, \phi) = 2E_0 - E_2 - E_4 = 4\sin^2\left(\Theta_{24}/2\right) \quad (8)$$

$$E_{2d}^{\pi/2}(\theta, \phi) = 2E_0 - E_5 - E_6 = 4\sin^2\left(\Theta_{56}/2\right) \quad (9)$$

By (7), (8) and (9), the response of second-order steered dipole (oriented toward φ_s) can be derived as

$$\begin{aligned}
&E_{2d}^{\varphi_s}(\theta, \phi) \\
&= \cos 2\varphi_s E_{2d}^{0}(\theta, \phi) + \sin 2\varphi_s E_{2d}^{\pi/4}(\theta, \phi) \\
&\quad + \frac{1}{2}\left(1 - \sin 2\varphi_s - \cos 2\varphi_s\right)\left[E_{2d}^{0}(\theta, \phi) + E_{2d}^{\pi/2}(\theta, \phi)\right] \\
&= 4\left[\cos 2\varphi_s \sin^2\left(\Theta_{31}/2\right) + \sin 2\varphi_s \sin^2\left(\Theta_{24}/2\right)\right] \\
&\quad + 2\left(1 - \sin 2\varphi_s - \cos 2\varphi_s\right)\left[\sin^2\left(\Theta_{31}/2\right) + \sin^2\left(\Theta_{56}/2\right)\right]
\end{aligned} \quad (10)$$

For $\Omega \ll 1$, we have $\sin^2(\Theta_{31}/2) \approx \Theta_{31}^2/4$, $\sin^2(\Theta_{24}/2) \approx \Theta_{24}^2/4$ and $\sin^2(\Theta_{56}/2) \approx \Theta_{56}^2/4$. Therefore, (10) can be reduced to

$$\begin{aligned}
&E_{2d}^{\varphi_s}(\theta, \phi) \\
&\approx \Omega^2 \sin^2\theta\Big\{\cos 2\varphi_s \cos^2\phi + \sin 2\varphi_s \cos^2(\phi - \pi/4) \\
&\quad + \frac{1}{2}\left(1 - \sin 2\varphi_s - \cos 2\varphi_s\right)\left[\cos^2\phi + \cos^2(\phi - \pi/2)\right]\Big\} \\
&= \Omega^2 \cos^2(\phi - \varphi_s)\sin^2\theta.
\end{aligned} \quad (11)$$

ISBN 978-0-9928626-7-1 © EURASIP 2017

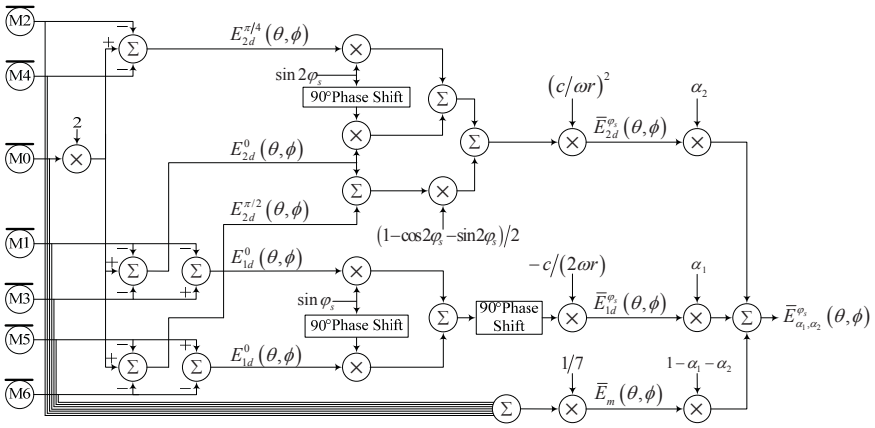

Fig. 2. Implementation structure of the proposed second-order steerable DMAs.

Furthermore, by normalizing the array response, we have

$$\overline{E}_{2d}^{\varphi_s}(\theta,\phi)=\frac{1}{\omega^2}\left(\frac{c}{r}\right)^2 E_{2d}^{\varphi_s}(\theta,\phi)\approx\cos^2(\phi-\varphi_s)\sin^2\theta. \tag{12}$$

where $1/\omega^2$ is a second-order integrator and $(c/r)^2$ is a compensation term.

3. THEORETICAL ANALYSIS

In this section, the DF and WNG of the proposed SOSDAs are analyzed theoretically. Due to the space limit, the theoretical derivations have been omitted in the following.

3.1. DF

For spherically isotropic diffuse noise, the DF is defined by

$$Q=\frac{4\pi|E_{\alpha_1,\alpha_2}^{\varphi_s}(\frac{\pi}{2},\varphi_s)|^2}{\int_{\phi=0}^{2\pi}\int_{\theta=0}^{\pi}|E_{\alpha_1,\alpha_2}^{\varphi_s}(\theta,\phi)|^2\sin\theta d\theta d\phi}. \tag{13}$$

Proposition 2: The DF of SOSDAs with its mainlobe oriented toward φ_s is given by

$$Q(\alpha_1,\alpha_2)\approx\frac{15}{20\alpha_1^2+8\alpha_2^2-30\alpha_1-20\alpha_2+20\alpha_1\alpha_2+15}. \tag{14}$$

By (14), we can see that the DF of SOSDAs is independent of the steering direction and also frequency-invariant. For the SOSDA with second-order cardioid response we have $Q=7.5$, while for that with second-order hypercardioid response we have $Q=9$. These DF values are exactly corresponding to those of their non-steerable counterparts.

3.2. WNG

To proceed, assume that the microphone signals E_i are all contaminated with sensor noise n_i, i.e.,

$$E_i^{(n)}(\theta,\phi)=E_i(\theta,\phi)+n_i(\theta,\phi). \tag{15}$$

With (15), the response of SOSDAs with sensor noise can be rewritten in a matrix form as

$$\overline{E}_{\alpha_1,\alpha_2}^{(n),\varphi_s}(\theta,\phi)=\mathbf{H}[\mathbf{E}(\theta,\phi)+\mathbf{N}(\theta,\phi)] \tag{16}$$

where $\mathbf{E}=[E_0,E_1,\ldots,E_6]^T$, $\mathbf{N}=[n_0,n_1,\ldots,n_6]^T$, with the superscript T being the transpose operator, and $\mathbf{H}(\Omega,\varphi_s)=\big[\varpi+\frac{2\alpha_2}{\Omega^2}\,,\varpi-\frac{\alpha_1}{2j\Omega}\cos\varphi_s-\frac{\alpha_2}{\Omega^2}(\cos 2\varphi_s+\iota),\varpi-\frac{\alpha_2}{\Omega^2}\sin 2\varphi_s,\varpi+\frac{\alpha_1}{2j\Omega}\cos\varphi_s-\frac{\alpha_2}{\Omega^2}(\cos 2\varphi_s+\iota),\varpi-\frac{\alpha_2}{\Omega^2}\sin 2\varphi_s,\varpi+\frac{\alpha_1}{2j\Omega}\sin\varphi_s-\frac{\alpha_2}{\Omega^2}\iota,\varpi-\frac{\alpha_1}{2j\Omega}\sin\varphi_s-\frac{\alpha_2}{\Omega^2}\iota\big]$. Herein, $\iota=\frac{1}{2}(1-\cos 2\varphi_s-\sin 2\varphi_s)$, and $\varpi=\frac{1}{7}(1-\alpha_1-\alpha_2)$.

WNG is defined as the array gain against spatially white noise, which is a commonly used measure for the robustness of beamformers [1]. When the temporally and spatially white noise with the same variance at all microphones, the WNG can be computed as

$$G_{wn}(\Omega,\theta,\varphi_s)=\frac{|\mathbf{H}(\Omega,\varphi_s)\mathbf{E}(\theta,\varphi_s)|^2}{\mathbf{H}(\Omega,\varphi_s)\mathbf{H}^T(\Omega,\varphi_s)}. \tag{17}$$

Substituting $\mathbf{E}$ and $\mathbf{H}$ in (15) into (17) and performing some approximation, we obtain the following proposition.

Proposition 3: The WNG of the proposed SOSDAs can be deduced as

$$G_{wn}(\Omega,\theta,\varphi_s)=\frac{\left[\alpha_1(1-\sin\theta)+\alpha_2\cos^2\theta+\frac{\varpi\Omega^2\sin^2\theta}{2}(3+\sin 2\varphi_s)-1\right]^2}{7\varpi^2+\frac{1}{\Omega^4}[6\alpha_2^2-2\alpha_2^2\sin 2\varphi_s(1-\sin 2\varphi_s)]+\frac{\alpha_1^2}{2\Omega^2}} \tag{18}$$

By (18), we can see that the properties of WNG are quite different from those of DF. The WNG of SOSDA is no longer frequency-invariant, and is an increasing function of Ω ($\Omega=2\pi fr/c$), and hence an increasing function of signal frequency f and the array size r. In addition, unlike the property of DF, the WNG is dependent on the steering angle φ_s.

ISBN 978-0-9928626-7-1 © EURASIP 2017

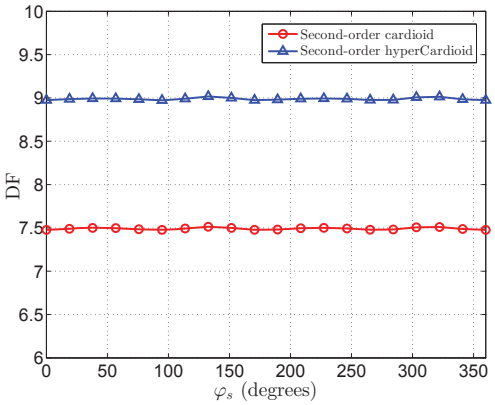

Fig. 3. DF of the proposed SOSDAs versus φ_s, where $\Omega = \pi/16$.

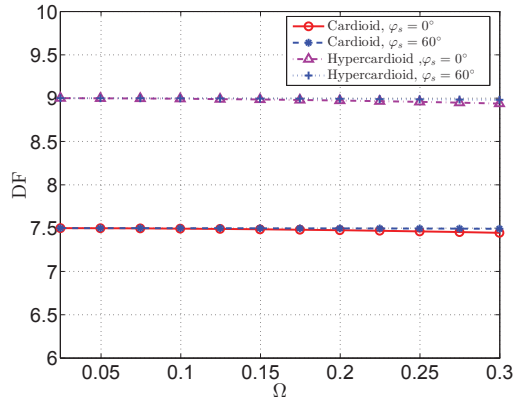

Fig. 4. DF of the proposed SOSDAs versus Ω.

Moreover, similar to the properties of non-steerable DMAs, although the DF values of SOSDA are higher than those of first-order counterparts, it is at the cost of low WNG.

4. NUMERICAL EVALUATION

In this section, we present some simulation results to demonstrate the effectiveness of the proposed SOSDA design. For ease of analysis, we assume that $\theta = 90°$ in the following.

Fig. 3 shows the DF of the proposed SOSDAs as a function of the steering direction φ_s for two types of array responses, i.e., second-order cardioid ($\alpha_1 = \alpha_2 = 1/2$) and second-order hypercardioid ($\alpha_1 = 1/3$ and $\alpha_2 = 5/6$), where $\Omega = \pi/16$. As we can see from Fig. 3, the DF of the SOSDAs is nearly independent on the steering directions, which is well consistent with the theoretical analysis. For second-order cardioid response, its DF maintains around 7.5, while for second-order hypercardioid response, its DF maintains around 9. In Fig. 4, the DF of the proposed SOSDAs

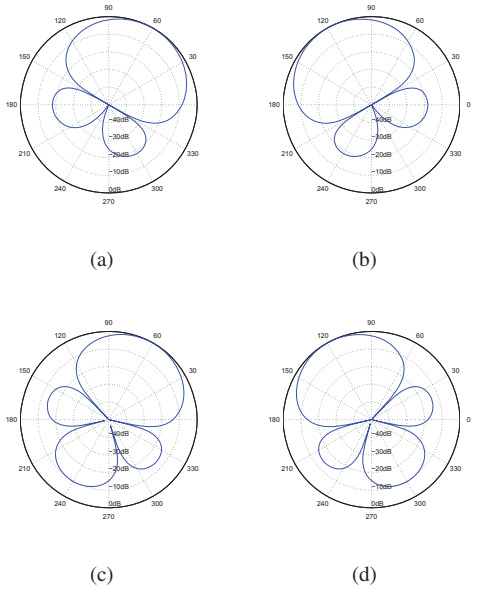

Fig. 5. Beampatterns of the SOSDAs with $\Omega = \pi/16$. (a) second-order cardioid with $\varphi_s = 60°$. (b) second-order cardioid with $\varphi_s = 120°$. (c) second-order hypercardioid with $\varphi_s = 60°$. (d) second-order hypercardioid with $\varphi_s = 120°$.

with various values of Ω is plotted, where two steering directions have been considered, i.e., $\varphi_s = 0°$ and $60°$. Similar to the theoretical result, the DF of the SOSDAs is shown independent on Ω, and thus also independent on signal frequency, for small values of Ω.

In Fig. 5, the beampatterns of the proposed SOSDAs are shown for the second-order cardioid and hypercardioid array responses, with $\Omega = \pi/16$. Figs. 5(a) and 5(b) are corresponding to the second-order cardioid response with $\varphi_s = 60°$ and $120°$, respectively. And Figs. 5(c) and 5(d) are corresponding to the second-order hypercardioid response with $\varphi_s = 60°$ and $120°$, respectively. From Fig. 5, we can see that the proposed SOSDAs can achieve beampattern rotation to desired directions perfectly.

Next, we study the WNG of the proposed SOSDAs. Fig. 6 shows the WNG of the proposed SOSDAs as a function of Ω, with $\varphi_s = 0°$. Again, two types of SOSDAs with the second-order cardioid and hypercardioid array responses are considered. For comparison, the WNG of the conventional non-steerable second-order DMAs (SODMAs) is also shown therein. It can be seen from the simulation results that the WNG of the SOSDAs is basically equal to that of the non-steerable SODMAs. Moreover, as revealed by the theoretical analysis, the WNG of the SOSDAs is indeed an increasing function of Ω. In Fig. 7 the WNG of the proposed SOSDAs is shown as a function of steering direction, where $\Omega = \pi/16$. Unlike the DF, we can see that the WNG of the SOSDAs is no longer frequency-invariant, which agree well with the the-

ISBN 978-0-9928626-7-1 © EURASIP 2017

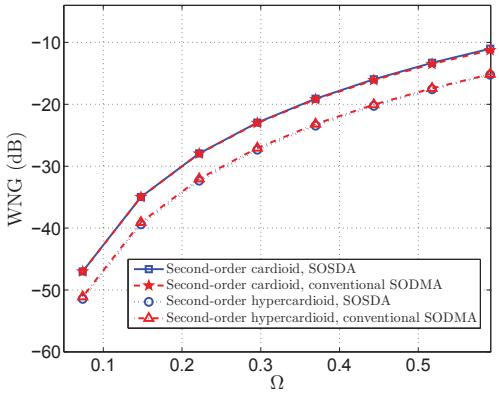

Fig. 6. WNG comparison of the proposed SOSDAs and the conventional second-order non-steerable DMAs (SODMAs). For the SOSDAs, φ_s is set to 0°.

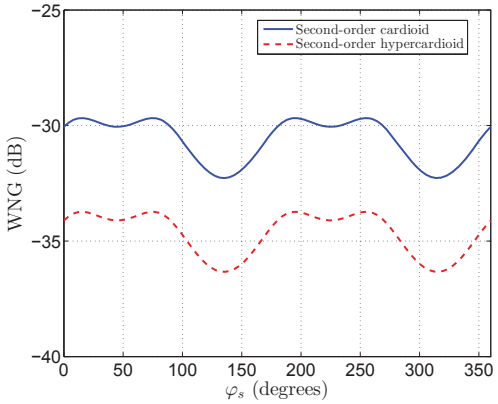

Fig. 7. WNG of the proposed SOSDAs versus φ_s, where $\Omega = \pi/16$.

oretical analysis.

5. CONCLUSION

In this paper, we have presented an approach for the design of second-order steerable DMAs, which can achieve beampattern rotation to arbitrary directions over the whole azimuthal space. Theoretical analysis on the DF and WNG of the proposed SOSDAs is given, and some related properties are also revealed. The effectiveness of the proposed design and its analysis has been further demonstrated via simulation results. In our future work, we will study the effect of microphone mismatches as well as sensor self-noise on the SOSDAs.

6. REFERENCES

[1] J. Benesty and J. Chen, *Study and Design of Differential Microphone Arrays,* Springer, 2013.

[2] G. W. Elko and A. T. N. Pong, "A simple first-order differential microphone," in *Proc. WASPAA,* Oct. 1995, pp. 169–172.

[3] H. Teutsch and G. W. Elko, "First- and second-order adaptive differential microphone arrays," in *Proc. IWAENC,* pp. 35–38, 2001.

[4] M. Ihle, "Differential microphone arrays for spectral subtraction," in *Proc. IWAENC,* pp. 259–262, 2003.

[5] T. D. Abhayapala and A. Gupta, "Higher order differential-integral microphone arrays," *J. Acoust. Soc. Amer.,* vol. 127, pp. EL227–EL233, 2010.

[6] E. De Sena, H. Hacihabiboğlu, and Z. Cvetković, "On the design and implementation of higher order differential microphones," *IEEE Trans. Audio Speech Lang. Process.,* vol. 20, pp. 162–174, 2012.

[7] L. Zhao, J. Benesty, and J. Chen, "Design of robust differential microphone arrays," *IEEE/ACM Trans. Audio Speech Lang. Process.,* vol. 22, pp. 1455–1465, 2014.

[8] C. Pan, J. Chen, and J. Benesty, "Theoretical analysis of differential microphone array beamforming and an improved solution," *IEEE/ACM Trans. Audio Speech Lang. Process.,* vol. 23, pp. 2093–2105, 2015.

[9] G. W. Elko and A. T. N. Pong, "A steerable and variable first-order differential microphone array," in *Proc. ICASSP,* pp.: 223-226, 1997.

[10] B. De Schuymer and H. Brouckxon, "Steerable microphone array system with a first order directional pattern," European Patent Appl., Appl. No.: 10151106.1, Aug. 24, 2011.

[11] R. M. M. Derkx and K. Janse, "Theoretical analysis of a first-order azimuth-steerable superdirective microphone array," *IEEE Trans. Audio Speech Lang. Process.,* vol. 17, pp. 150–162, 2009.

[12] X. Wu, H. Chen, J. Zhou, and T. Guo, "Study of the mainlobe misorientation of the first-order steerable differential array in the presence of microphone gain and phase errors," *IEEE Signal Process. Lett.,* vol. 21, pp. 667–671, 2014.

[13] X. Wu and H. Chen, "Directivity Factors of the First-Order Steerable Differential Array With Microphone Mismatches: Deterministic and Worst-Case Analysis", *IEEE/ACM Trans. Audio Speech Lang. Process.,* vol. 24, pp. 300–315, 2016.

ISBN 978-0-9928626-7-1 © EURASIP 2017